Transactions of the Korean Nuclear Society Autumn Meeting
Yeosu, Korea, October 25-26, 2018

Using the Spark Plasma Sintering (SPS) System for the High Temperature Creep Behavior Evaluation of NbMoTiVSi Alloy

Faris B. Sweidan[a], Ho Jin Ryu[a*]
[a] *Department of Nuclear and Quantum Engineering, KAIST, Yuseong-gu, Daejeon 34141, Republic of Korea*
**corresponding author: hojinryu@kaist.ac.kr*

1. Introduction

During pressure assisted sintering, which is also known as Spark Plasma Sintering (SPS), a correlation between the densification kinetics and the compressive creep has been noticed and analyzed [1-3]. This was due to the fact that creep of ceramics was the main mechanism occurring in the densification final stage. Therefore, creep parameters of the materials during the sintering process were noted and recorded. After the analysis, it was found that these parameters were in good agreement with those obtained from conventional creep experiments.

In that sense, an SPS apparatus has been used as an accurate high-temperature creep testing system in several recent studies [4-6]. The creep test has been conducted through a special SPS graphite mold configuration. In this study, the configuration consists of graphite dies, Al_2O_3 disks that act as insulators, and WCrTaV high entropy alloy (HEA) disks as support between the sample and the Al_2O_3 disks. Fig.1 shows the graphite mold configuration for the SPS creep test.

According to the studies [4-6], the setup was capable to be used for creep tests of metals and ceramics and it provides accurate output data, including temperature, pressure, and relative punch displacement (RPD) as well as electric field parameters. The results, extrapolated to higher temperatures and lower stresses, were in good agreement with data reported in the literature.

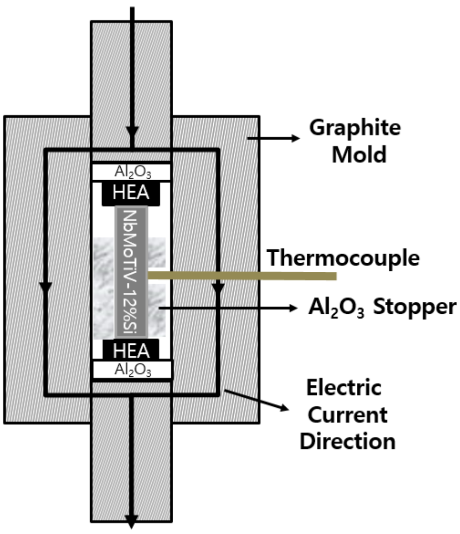

Fig. 1. The SPS mold setup for the creep test.

In the authors' previous work [7], the procedure of performing uniaxial compressive creep tests using an SPS apparatus was presented. In this study, the optimization of that experimental procedure and the creep behaviour of NbMoTiV-12%Si alloy, tested by the SPS system at a temperature of 1200 ºC and a pressure of 200 MPa, are discussed.

2. Experimental Procedure

A significant concern when conducting the creep tests using SPS is the effect of an electromagnetic field within the SPS apparatus. Generally, a relatively low voltage (≤10 V) is applied to the whole setup, while a very high electric current is employed (1–10 kA) [3]. For conductive materials, the high current significantly affects creep behavior, with this being attributed to the effects of electro-plasticity. Therefore, an isolating material can be used between the testing sample and the mold punches to avoid passing the current through the sample. In this study, Al_2O_3 disks are used as an insulator.

In our previous experiments, the Al_2O_3 disks suffered bending in the contact area between the sample and the disk. Therefore, a supporting material is necessary. In this case, WCrTaV high entropy alloy was chosen as it showed superior properties in terms of strength and hardness [8]. Therefore, the actual experimental procedure starts with fabricating the WCrTaV high entropy alloy disks. The composition of this alloy is as follows [8]: 39.37 wt.% W, 10.91 wt.% V, 38.75 wt.% Ta, and 10.97% Cr. The powders and steel balls were put in a plastic bottle with 1:1 mass ratio to be mixed at 30 rpm for 24 hours. The mixed powder was sintered using SPS at 1500 ºC and 50 MPa for 10 mins. The resulting WCrTaV high entropy alloy disks were used as a support material between the sample and the insulating material. For the temperature measurement, an R-type thermocouple and a pyrometer were used.

3. Theory

Temperature, pressure (force), and displacement are the parameters of the major significance. The displacement results can be analyzed to calculate the strain and the creep strain rate. Repeating the experiment at different temperatures and pressures leads to the calculations of the activation energy and the stress component, respectively, according to the following equation [1,4,5]:

$$\dot{\varepsilon} = A\sigma^{n} \exp\left(\frac{-Q}{RT}\right) \quad \ldots (1)$$

where $\dot{\varepsilon}$ is the creep rate, A is the creep constant, σ is the applied load, n is the stress exponent, Q is the activation energy, R is the gas constant and T is the temperature.

4. Results

After the optimization of the experimental setup and procedure of the creep test using the SPS system, NbMoTiV-12%Si alloy sample has been tested. The sample dimensions are 4.3 mm in diameter and 7 mm in height. The test was conducted at a temperature of 1200 ºC under a pressure of 200 MPa for 30 mins.

4.1 SPS System Readings: Temperature, Pressure, and Displacement

Temperature, pressure (force), and displacement are the major parameters that are required for the creep test. Fig. 2, Fig. 3, and Fig. 4 show the temperature, pressure, and displacement readings of the SPS system, respectively.

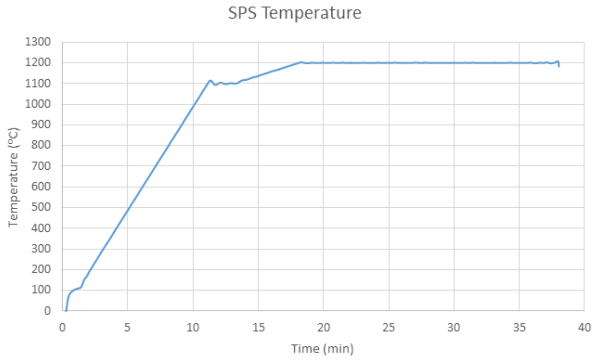

Fig. 2. Thermocouple temperature reading of the creep test.

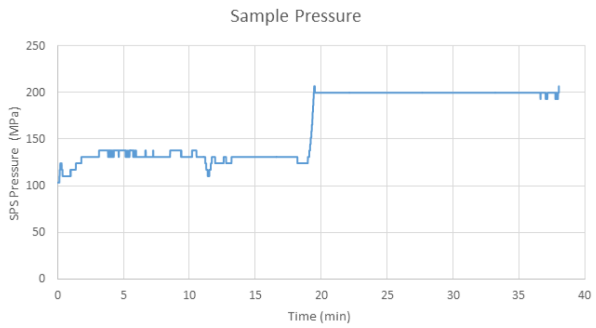

Fig. 3. Sample pressure reading of the creep test.

It is worth mentioning that in the beginning of the experiment, the sample experiences thermal expansion and the SPS Relative Punch Displacement (RPD) reading gives a negative value while the sample pressure increases. After reaching a certain temperature during the heating, the punches relative displacement reading starts to increase and the pressure reading decreases as the sample starts to deform. Therefore, the thermal expansion effect should be taken into account in the strain and strain rate calculations.

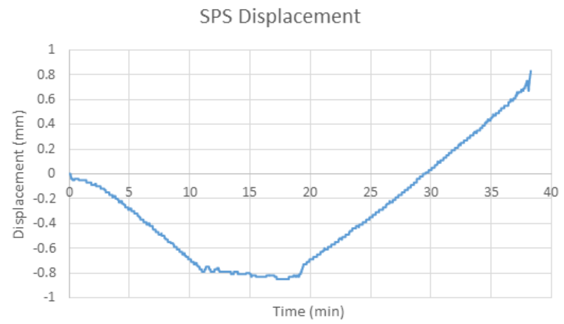

Fig. 4. Displacement reading of the creep test.

4.2 Displacement Mechanical Equilibrium, Engineering Strain, and True Strain

To take the thermal expansion effect into account, the minimum RPD reading is considered point zero in the displacement and the resulting strain curves. In that sense, Fig. 5 and Fig. 6 show the displacement after the thermal expansion effect and the true strain, respectively. The true strain was calculated through the following equation:

$$\text{True strain} = \ln\left(\frac{h_0}{h}\right) = -\ln(1 - [\text{engineering strain}]) \quad \ldots (2)$$

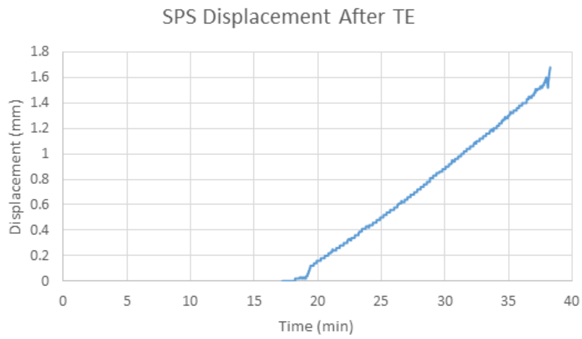

Fig.5. Displacement after the thermal expansion.

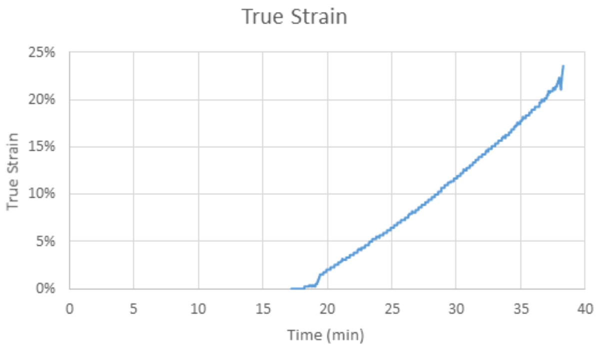

Fig.6. True strain with time.

As mentioned previously, the height of the sample before the test is 7 mm. The height of the resulting sample after the test is 5.6 mm. From the SPS displacement readings, the maximum displacement that the sample reached is 0.88 mm. Therefore, the resulting uncertainty of the displacement reading (through multiple experiments) is ~±0.5 mm. Fig. 7 shows the sample before and after the test.

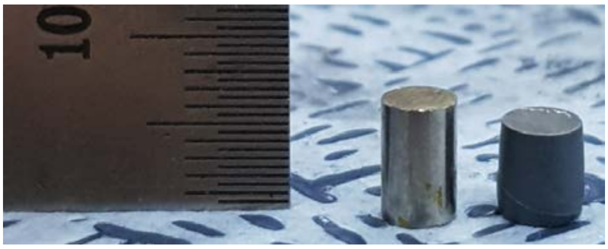

Fig.7. Sample before and after the test.

4.3 Steady-state Creep Rate Calculations

From the displacement readings with time of the SPS, the steady-state (secondary) creep strain rate can be calculated. Therefore, Fig. 8 shows the creep strain rate in log scale.

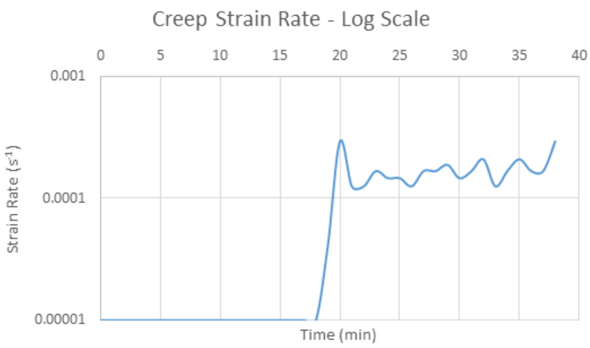

Fig.8. Creep strain rate in log scale.

The creep strain rate value is taken at 10% strain (around the 30 mins mark). This value is equal to 1.458 x 10^{-4} s^{-1}. It represents the steady-state creep rate of the tested alloy at a temperature of 1200 ºC and a pressure of 200 MPa.

4.4 Microstructure and Phase Composition Analysis

After the test, the sample was mounted and prepared for the microstructure analysis using SEM/EDS to evaluate the phases and the composition of the sample material. SEM, BS, and EDS were performed on the tested sample. Fig. 9 shows the microstructure of the tested sample at different locations and magnifications.

The microstructure shows that there are two phases: a dark phase and a bright phase. The EDS analysis identified the dark phase as a Si-rich phase while the bright phase with a lower Si content. The EDS analysis peaks for the two phases are shown in Fig. 10 including the weight and atomic fraction of each element in each phase.

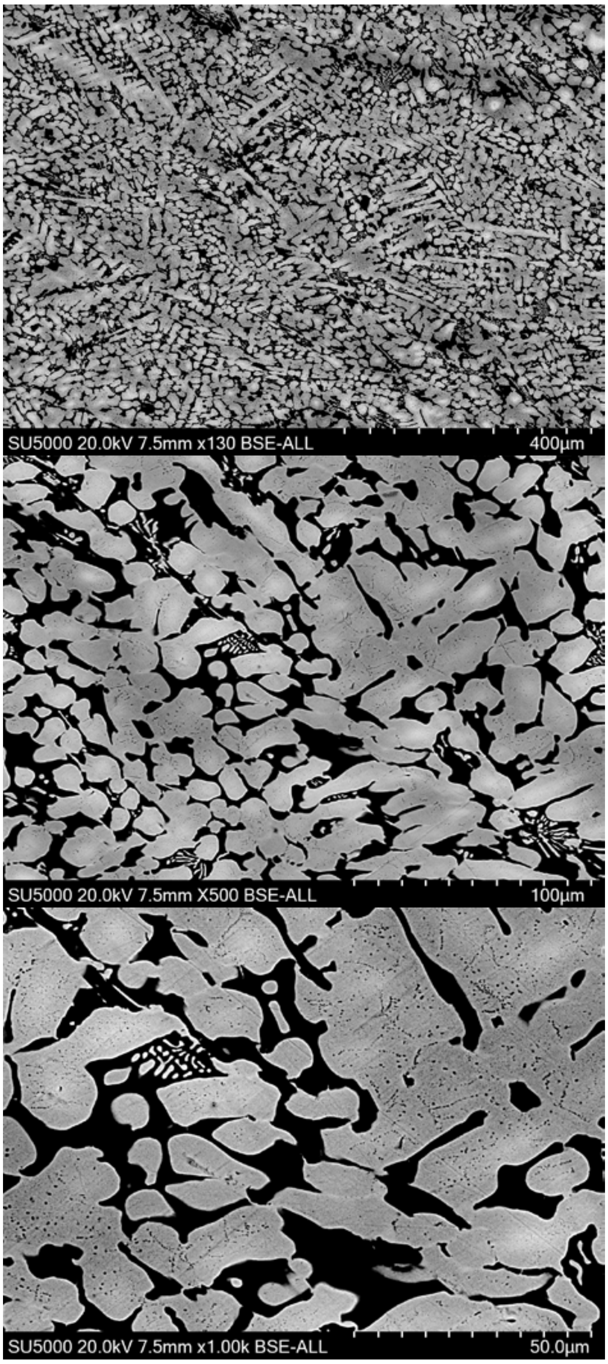

Fig.9. SEM images of the tested sample at different locations and magnifications.

5. Conclusion

In this study, the steady-state creep behavior of NbMoTiV-12%Si alloy has been evaluated using an SPS system after the optimization of the experimental setup and procedure. After that, the microstructure of the tested samples has been analyzed using SEM/EDS. Repeating the experiment at different temperatures and pressures leads to the calculations of the activation energy and the stress component, respectively, through Equation 1.

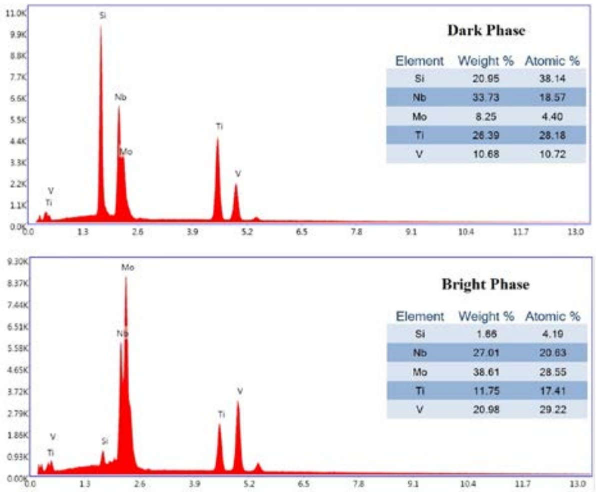

Fig.10. EDS Analysis peaks of the two phases.

Evaluating the creep performance data from SPS for metallic alloys as well as ceramics will give access to obtaining such missing properties of some materials that will be used in advanced nuclear fuel designs. As future work, this apparatus will be used to evaluate the high temperature creep behavior of more materials in wide temperature and pressure ranges.

ACKNOWLEDGMENTS

This study is supported by the Agency for Defense Development (ADD).

REFERENCES

[1] N. Chawake et al., "On correlation between densification kinetics during spark plasma sintering and compressive creep of B2 aluminides", Scripta Materialia 107 (2015) 63–66.

[2] R.L. Coble, "Diffusion models for hot pressing with surface energy and pressure effects as driving forces", Journal of Applied Physics, 41 (12) (1970) 4798–4807.

[3] D.S. Wilkinson, M.F. Ashby, "Pressure sintering by power law creep", Acta Metallurgica 23 (11) (1975) 1277–1285.

[4] Barak Ratzker et al., "Using a spark plasma sintering apparatus as a tool in a compressive creep study of fine-grained alumina", Ceramics International 43 (2017) 9369–9376.

[5] Barak Ratzker et al." Compression creep of copper under electric current studied by a spark plasma sintering (SPS) apparatus", Materials Science & Engineering A 712 (2018) 424–429.

[6] Barak Ratzker et al., "Creep of Polycrystalline Magnesium Aluminate Spinel Studied by an SPS Apparatus", Materials 2016, 9, 493.

[7] Faris B. Sweidan et al., "Compressive Creep Deformation Test Using a Spark Plasma Sintering (SPS) Apparatus", Transactions of the Korean Nuclear Society, Spring Meeting, Jeju, Korea, May 2018.

[8] Owais Ahmed Waseem et al., "The effect of Ti on the sintering and mechanical properties of refractory high-entropy alloy TixWTaVCr fabricated via spark plasma sintering for fusion plasma-facing materials", Materials Chemistry and Physics 210 (2018) 87-94.